A Sensor-Based Unit for Diagnostics and Optimization of Solar Panel Installations

Lasse Berntzen[1(✉)], Saeed Teimourzadeh[2], Paula Anghelita[3], Qian Ming[1], and Viorel Ursu[3]

[1] University of South-Eastern Norway, Kongsberg, Norway
lasse.berntzen@usn.no
[2] EPRA Electric Energy Co, Ankara, Turkey
[3] ICPE, Bucharest, Romania

Abstract. To solve the problem of relatively low efficiency in most of nowadays solar panels, this paper proposes a new solution by diagnosing and optimizing solar panel installations. Dr. Solar, a sensor-based device, acquires information on solar radiation, geographical position, inclination, roll, panel temperature, and ambient temperature and humidity. The sensor-based device is mounted to the solar panel for a few days while collecting data. The cloud-based service gathers information from the inverter while the device is moved to other installations. Combined with the data of power generation from the inverter, a cloud service is offered for processing and analyzing the data to maximize power production by adjusting the panel installation. During several short-term experiments in different places, Dr. Solar provided reliable data for analysis on the cloud platform, and a web interface was developed to calculate power production. The solution has increased photovoltaic panels' efficiency by optimizing adjustments to the panel's physical position (tilt and angle). The paper describes the sensor-based device, the cloud service, and the algorithms used.

Keywords: photovoltaic energy · solar panels · optimization · diagnostics · big data · analytics · sensors · Dr. Solar

1 Introduction

Photovoltaic energy has just reached a new dimension. According to the research of SolarPower Europe, in May 2022, the total global installed solar capacity has passed the 1 TW threshold [1]. That is 500 times increase compared to 2002, when the capacity was only 2 GW. It took 16 years, until 2018, to reach the 500 GW level, and only three years later, the amount has doubled to 1,000 GW or 1 TW. The forecast for the rest of 2022 shows an increase of 200 GW in one year. Solar power has become the third most significant renewable energy source by installed capacity, after hydro and wind power [1].

At the same time, however, solar still meets only a small share of around 4% of the global electricity demand, while non-renewable sources provide over 70%. In 2022, global solar additional installation capacity expects to increase by 36% to 228.5 GW.

The world will see solid demand for solar in the next four years, growing from 255.8 GW of additional capacity in 2023 to 347 GW in 2026. It will likely add 314.2 GW in 2025 [1].

Most commercial solar panels have efficiencies from 15% to 20% [2]. Therefore there is a demand to improve the efficiency of energy conversion. Although emerging perovskite solar cells have a high conversion efficiency (over 25%), there is still a long way for perovskite solar cells to get commercialized since perovskite crystals are easily decomposed in a humid environment. At the moment, the lack of stability is a significant disadvantage.

This paper reports on a project to diagnose and optimize the use of solar panel installations by developing a prototype sensor platform fixed to the panels and delivering data to a cloud-based service for analytics. The project was a collaborative effort between ICPE (Romania), EPRA (Turkey), and the University of South-Eastern Norway in 2021 and 2022. Photovoltaic panel output depends on several factors. The idea of Dr. Solar is to optimize the placement of the solar panels based on an analysis of such elements.

The essential characteristics of solar panels include the following:

- Structural characteristics (roof-top mounted, ground mounted, wall mounted)
- Type (monocrystalline, polycrystalline, thin film)
- Geographical position (latitude, longitude, altitude)
- Magnetic orientation, inclination, and base slop (roll)

Operational characteristics.

- Solar radiation level
- Solar panel back side temperature
- Ambient temperature
- Ambient relative humidity

The installation of the photovoltaic panels should consider some factors to make the most use of solar radiation: the material types, the geographical position, the elevation, inclination/angle, and solar radiation conditions. The correct measurement and adjustment of these factors ensure that photovoltaic panels produce maximum energy by being exposed to the greatest intensity of solar radiation during operation. Photovoltaic cells employ solar radiation in their operation; hence the cells are affected by the weather or condition of the atmosphere to which they are exposed. Here, the temperature is an essential factor which can be evaluated from two standpoints, i.e., ambient temperature and solar cell surface temperature. The electrical efficiency of solar cells depends on the ambient temperature. Solar cells are made of semiconductor materials like the most used crystalline silicon, and semiconductors are sensitive to temperature. Solar panels represent a negative temperature coefficient, and their performance declines when the temperature increases. The main reason is that an increment in the temperature decreases the band gap of a semiconductor which decreases the open circuit voltage of solar cells and the output power [3].

Regarding the cell surface temperature, the surface temperature can also be affected by the ambient temperature. However, the challenging point is the occurrence of hotspot

areas. Hot spots are areas of high temperature that affect a solar cell by consuming energy instead of generating it [4]. As the solar cells are connected in series, a weak cell or group of cells will affect the energy production of all the cells on the same string.

The other factor is humidity. Solar radiation is electromagnetic waves, and when the light consisting of photon strikes the water layer, which is denser, refraction appears and decreases the light's intensity. Because the efficiency depends upon the value of the maximum power point of the solar cell, the effect of humidity deviates from the maximum power point, decreasing solar cell efficiency [5].

Humidity readily affects the efficiency of the solar cells and creates a minimal layer of water on their surface. It also decreases the total power output produced. Panjwani et al. [6] conducted more than four experiments with water absorbents to improve efficiency and make the system more efficient.

The next section provides a conceptual description of the Dr. Solar system. The following sections describe data collection, data analysis, and results. Finally, the last section contains the conclusion and ideas for further work.

2   Conceptual Description

Dr. Solar is a system designed to assess photovoltaic systems by collecting relevant measurement parameters followed by an analysis in the cloud using dedicated algorithms that give indications for optimizing energy production. The system consists of the following main parts:

- Dr. Solar box containing various sensors
- The inverter that collects and provides the data concerning energy production
- A cloud-based platform that provides analytics service based on data obtained from the Dr. Solar box sensors and the inverter

The results from the cloud-based service are presented to the user as a report which contains, along with the presentation of the results regarding the configuration of the installed photovoltaic system, indications related to possible adjustments of the system to increase energy production. The inverter production-related problems are also included in the report. Figure 1 shows the main parts that compose the Dr. Solar solution.

The inverter transforms the DC low voltage gained from the solar panels into 220–240 V AC used in households. The prototype of the Dr. Solar device was used with a Huawei inverter SUN2000L-3KTL model to demonstrate the functionality.

The inverter collects and submits data about its input and output parameters, such as input and grid currents, input and grid voltages, active and reactive power, and energy production.

The Dr. Solar box also collects and uploads data into the same cloud-based platform, where analytics service is implemented using a GSM-based mobile router. A router is necessary since the solar panels are usually not placed in areas covered by Wi-Fi connection. The Dr. Solar box is set to collect data every 5 min for three consecutive days, ideally when radiation exceeds 600 W/m^2. Both the Dr. Solar device and inverter provide data at five minutes intervals that are polled by the cloud-based analytics service for the time interval between 10:00 am to 2:00 pm.
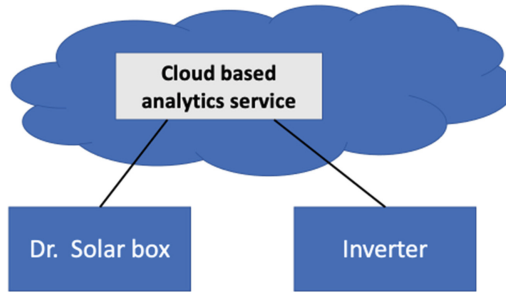
Fig. 1. The main components of Dr. Solar

3   Collecting Data

The Dr. Solar box is a sensor-based module designed to collect data from sensors and send them to the cloud platform to be processed. The Dr. Solar box is attached to the solar panel and stays there for a few days. The device can then be moved to a new location to collect and submit new data to be processed by the cloud service. The cost of the box does not justify a permanent mounting in only one location, except for large installations. During a few days, the Dr. Solar box will collect the data used for analytics. The sharing of the Dr. Solar box between many photovoltaic systems users justifies the costs of producing the sensors units/boxes.
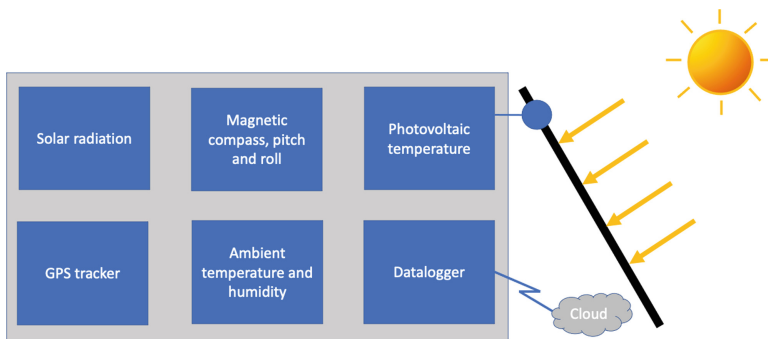
Fig. 2. Dr. Solar Box

Figure 2 shows the different building blocks of the Dr. Solar box. The Dr. Solar box includes several sensors relevant to photovoltaic systems investigation, as follows:

- Solar radiation
- Magnetic compass, inclination, and roll (base slope)
- Photovoltaic panel temperature (measures the back-side surface temperature of the solar panel)
- GPS tracker
- Ambient temperature and relative humidity

Figure 3 shows the prototype of the Dr. Solar device. The radiation sensor is on the top front view right side. The wire on the left side is for the surface temperature sensor.

Fig. 3. The Dr. Solar box

Figure 4 shows how the Dr. Solar device prototype mounted on the solar panel.

Fig. 4. The Dr. Solar box fixed to the solar panel

Table 1 briefly describes the different components of the Dr. Solar box. The components are also shown in Fig. 5

The controller is a data logger that also has a protocol stack. The data logger can be used as a web client and server. It is the datalogger that submits information to the cloud-based service.

Table 1. Dr. Solar box sensors

Sensor	Model	Description
Solar radiation sensor (pyranometer)	SR05-D1A3-PV	Measures solar radiation received by the plane surface
Temperature sensor	NTC 10k	Measures the surface temperature of the photovoltaic panel
Magnetic compass and inclinometer	DCS456M	This sensor is used to find the photovoltaic panel orientation and pitch. Together with the GPS, it provides positioning data for the prosumer-installed photovoltaic panels, useful for knowing the incident angle of the solar radiation
Temperature and humidity sensor	Lumel18D	A sensor that measures ambient temperature and relative humidity
GPS tracker	iUni GT02	GPS tracker has a built-in GSM module for mobile communication. The device is waterproof and mainly used for theft protection of cars and motorbikes. The GPS tracker is used to obtain the exact position of the photovoltaic panel
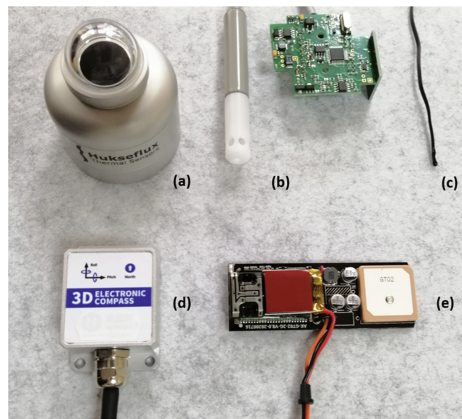
Fig. 5. Dr. Solar sensors: (a) Solar radiation sensor, (b) Ambient temperature and relative humidity sensor, (c) Photovoltaic panel temperature sensor, (d) Magnetic compass and inclinometer, (e) GPS tracker

4   Analyzing the Data

The analytics process is visualized in Fig. 6. The left side shows the Dr. Solar device and the inverter. The cloud-based service is in the middle, and the web-based user-interface is on the right.
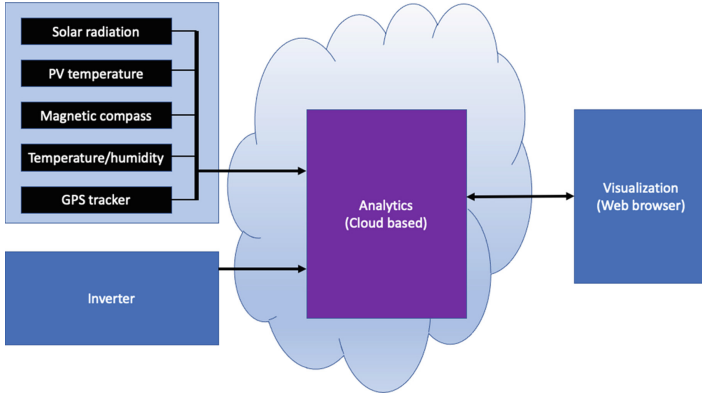

Fig. 6. The analytics process visualized

Dr. Solar is the implementation of an idea of a cloud-based analysis and diagnosis platform for photovoltaic prosumers, shortened as (PVADIP-C). The proposed platform provides a cost-effective solution for small on-grid photovoltaic systems. The relevant onsite data are collected and sent to a dedicated cloud platform to be processed, analyzed, and diagnosed. Hence, there is no need to implement expensive control and optimization engines at small-scale photovoltaic locations. Two main functionalities are envisioned for the PVADIP-C. The outline of the proposed method is depicted in Fig. 7. As can be seen, the first functionality is an operational decision-making engine that optimizes a photovoltaic-based prosumer's operation. The second engine is the asset management engine which identifies the possible failures in the photovoltaic-based prosumer.

4.1   Operational Decision Support

This section deals with a small-scale photovoltaic system proposed operational decision support mechanism. Figure 8 depicts a schematic of a load point which includes a connection to the upstream grid, small-scale photovoltaic system, fixed loads, controllable loads (washer & dryer, dishwasher, and pump), storage device, and plug-in electric vehicle.

For optimal operation, the objective is minimum cost while satisfying technical constraints pertaining to nodal power balance, power transactions with the upstream network, and permissible operation range of elements.

The objective function can be formulated as follows:

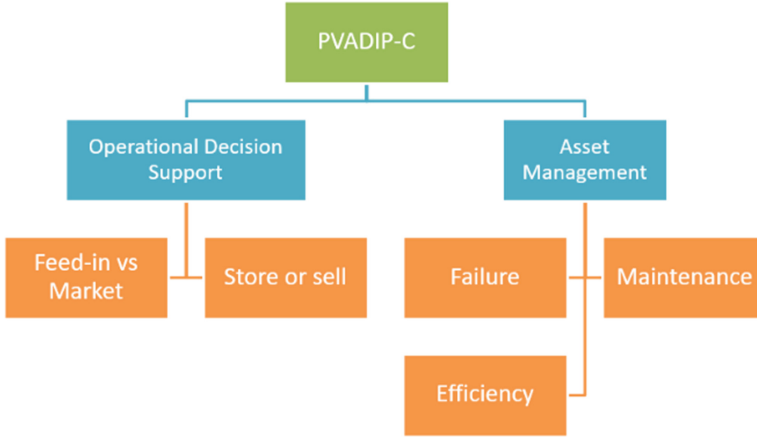$$Minimize\ OF = \sum_{t \in I_T} \left(\lambda_t^{Buy} P_t^{Buy} - \lambda_t^{Sell} P_t^{Sell} \right) \tag{1}$$

Fig. 7. Outline of the proposed methodology for PVADIP-C
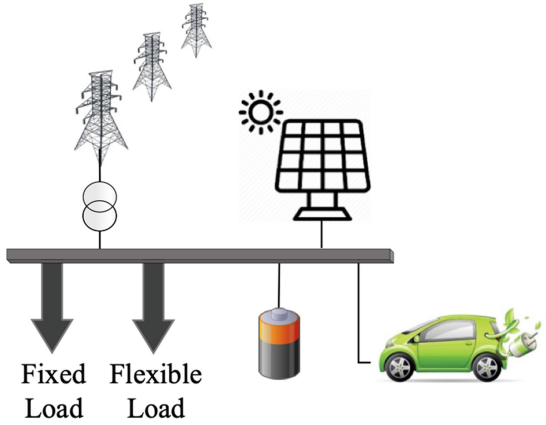

Fixed Flexible
Load   Load

Fig. 8. Schematic of a load point with a small-scale photovoltaic system, flexible loads, and storage devices

t, I_T I ndex and set of time
Buy, Sell Superscript for buying from and selling to the market
P Active power
λ Price per kilowatt

The primary constraint is to maintain nodal power balance, which is formulated as follows:

$$P_t^{Gen} - P_t^{Load} = 0 \quad \forall t \in I_T \tag{2}$$

$$P_t^{Gen} = P_t^{Buy} + P_t^{PV} + P_t^{Bat-} + P_t^{EV-} \quad \forall t \in I_T \tag{3}$$

$$P_t^{Load} = P_t^{Sell} + P_t^{Fix} + P_t^{Flex} + P_t^{Bat+} + P_t^{EV+} \quad \forall t \in I_T \tag{4}$$

PV, *Bat*, *EV*, *Fix*, *and Flex* are superscripts for solar generation, plug-in electrical vehicles, fixed load at home, and flexible load at home, respectively. Here, $+$ and $-$ superscripts show the charging\discharging stage of battery storage and plug-in electric vehicle, respectively.

The technical constraints for small-scale photovoltaic operation are represented by (5)–(23). The power transacted between the load point and upstream network should be within a pre-defined range modeled by (5) and (6).

$$0 \leq P_t^{Buy} \leq \alpha_t^M P_t^{Buy,Max} \tag{5}$$

$$0 \leq P_t^{Sell} \leq \left(1 - \alpha_t^M\right) P_t^{Sell,Max} \tag{6}$$

M is the symbol for market-related quantities, *Min* and *Max* are symbols for lower and upper limits, respectively. In (5) and (6), the binary variable is used to avoid enabling both selling and buying options simultaneously. The upper and lower limits of photovoltaic generation are modeled by (7)

$$P_t^{PV,Min} \leq P_t^{PV} \leq P_t^{PV,Max} \tag{7}$$

The state-of-charge (SOC) of the storage device at each period is calculated by (8) [7]. Constraint (10) is limitations on SOC, and (11)–(12) is limitations on charge/discharge power associated with storage.

$$SoC_t^{Bat} = SoC_{(t-1)}^{Bat} + \frac{\eta^{Bat} \Delta t}{E^{Bat,Max}} \left(P_{(t-1)}^{Bat+} - (\eta^{Bat})^{-2} P_{(t-1)}^{Bat-}\right) \tag{8}$$

$$SoC^{Bat,Min} \leq SoC_t^{Bat} \leq SoC^{Bat,Max} \tag{9}$$

$$0 \leq P_t^{Bat+} \leq \alpha_t^{Bat} P^{Bat+, Max} \tag{10}$$

$$0 \leq P_t^{Bat-} \leq \eta^{Bat} \left(1 - \alpha_t^{Bat}\right) P^{Bat-, Max} \tag{11}$$

η is the conversion efficiency coefficient, α is a binary decision variable, and E is the energy capacity for the storage unit. The EV charge/discharge constraints are modeled by (12)-(13) associated with storage. In (14), the SOC of parking lots in various time intervals is computed. Constraints on the target SOC of parking lots are stated by (15)-(17), respectively.

$$0 \leq P_t^{EV+} \leq \alpha_t^{EV} P^{EV+,Max} \tag{12}$$

$$0 \leq P_t^{EV-} \leq \eta^{EV} \left(1 - \alpha_t^{EV}\right) P^{EV-,Max} \tag{13}$$

$$SoC_t^{EV} = SoC_{(t-1)}^{EV} + \frac{\eta^{EV} \Delta t}{E^{EV,Max}} \left(P_{(t-1)}^{EV+} - (\eta^{EV})^{-2} P_{(t-1)}^{EV-}\right) \tag{14}$$

$$SoC^{EV,Min} \leq SoC_t^{EV} \leq SoC^{EV,Max} \tag{15}$$

$$0 \leq P_t^{EV+} \leq \alpha_t^{EV} P^{EV+,Max} \left(1 - SoC_t^{EV}/1 - SoC_t^{Sat-EV}\right) \tag{16}$$

$$0 \leq P_t^{EV-} \leq \left(1 - \alpha_t^{EV}\right) P^{EV-,Max} \left(1 - SoC_t^{EV}/1 - SoC_t^{Sat-EV}\right) \tag{17}$$

Equations (18)–(23) model controllable loads as follows:

$$P_t^{Flex} = \alpha_t^{Flex} P^{Flex,Dep} \tag{18}$$

$$\sum_{t \in I_T} \alpha_t^{Flex} = T^{Flex} \tag{19}$$

$$\alpha_t^{Flex} - \alpha_{t-1}^{Flex} = \beta_t^{Flex} - \zeta_t^{Flex} \quad \forall t \in [2, 24] \tag{20}$$

$$\sum_{i=t-T^{Flex}+1}^{t} \beta_i^{Flex} \leq \alpha_t^{Flex} \quad \forall t \in \left[T^{Flex} + 1, 24\right] \tag{21}$$

$$\sum_{i=t-DT^{Flex}+1}^{t} \zeta_i^{Flex} \leq 1 - \alpha_t^{Flex} \quad \forall t \in \left[DT^{Flex} + 1, 24\right] \tag{22}$$

$$DT^{Flex} = 24 - T^{Flex} \tag{23}$$

Dep is superscript for deployment, T is the time required for the complete operation of the equipment and are auxiliary binary variables. Equation (18) expresses that the power consumed by the flexible load at time t, i.e., is equal to its nominal power consumption while deployment if it is in operation, i.e., otherwise, is 0. In addition, the operation time of a flexible load should be equal to the required time for its complete operation, modeled by (19). Here, continuous operation of flexible load should also be considered. In other words, when the flexible load is committed, it should be continuously in operation until the time required for its complete operation (interruption is not allowed). To this end, the suit of constraints represented by (20)–(23) is added.

The outputs of the optimization engine are:

- Optimal amount of photovoltaic-based generation to be consumed at each hour.
- Optimal amount of power to be traded with the upstream network.
- Optimal charging\discharging pattern for battery storage and electric vehicle.
- Optimal commitment of controllable loads.
- Hourly cost of community operation.

The required inputs for the proposed model are:

- Hourly energy price (\$/kWh).
- Hourly fix load (kW).
- Hourly generation of the photovoltaic generation (kW).
- Installed capacity for renewable generation, battery storage, and electric vehicle.

- Permissible operating range of devices.

From the inputs mentioned above, the hourly fix load and the photovoltaic generation can be acquired from the Dr. Solar box. The user or the operator can enter additional information. With this data in place, the devised model offers the optimal operation for a load point equipped with a small-scale photovoltaic system. Note that Dr. Solar's optimal decision support service can be offered when Dr. Solar is installed for a considerable period at the customer's place, for instance, a month.

4.2 Asset Management

This section deals with devising an asset management approach for small-scale photovoltaic systems. The main objective is to detect any failure or deficiency that results in the efficient operation of a small-scale photovoltaic system. The outline of the proposed approach for asset management of small-scale photovoltaic systems is depicted in Fig. 9.
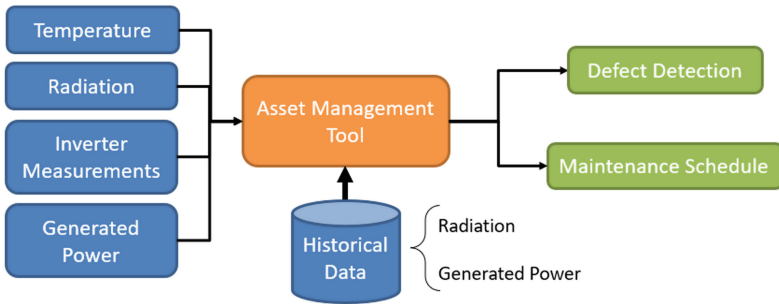
Fig. 9. Outline of the proposed approach for asset management

The main objective is to estimate the small-scale photovoltaic system's output power and ensure that all system elements are intact. The estimated output power is then compared with the measured power, and a failure occurrence is reported in case of substantial difference. Here, the proposed methodology calculates the DC side parameters for accurate decision-making. The detailed calculation within the asset management toolbox in Fig. 9 is depicted in Fig. 10.

In Fig. 10, three types of inputs are required. The first category is the measurement which is solar irradiation and ambient temperature. The second and third groups are the data on solar cells and the inverter, accessible through the data sheets. Once the input data are acquired, the next step is calculating the power at the DC side of the inverter. The DC power is calculated as [8]:

$$I_{mpp} = I_{mpp,ref} \frac{G}{G_{ref}} \tag{24}$$

$$V_{mpp} = V_{mpp,ref} \ln\left(e + c\left(G - G_{ref}\right)\right) \tag{25}$$
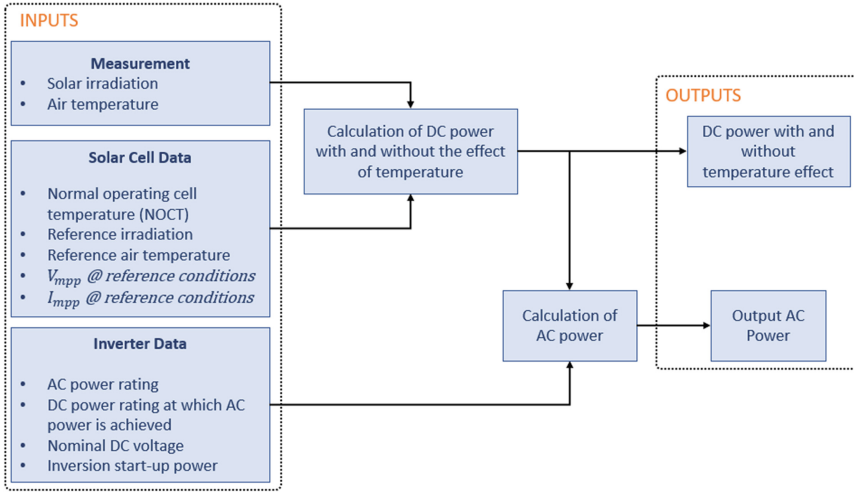
Fig. 10. The detailed calculation within the asset management toolbox

$$P_{DC} = V_{mpp}I_{mpp} \tag{26}$$

$I_{mpp, ref}$, and $V_{mmp, ref}$ is the current and voltage associated with maximum power point. G and G_{ref} are solar irradiation and associated reference value. P_{DC} is the output DC power, excluding the effect of ambient temperature. The DC power can be affected by the ambient temperature, which is considered. The cell temperature should be calculated as follows [9]:

$$T_c = T_{air} + \left(T_{NOCT} - T_{ref}\right)\frac{G}{G_{ref}} \tag{27}$$

T_{air} is the ambient temperature, T_{NOCT} is the normal operating cell temperature, and T_{ref} is the reference temperature. Once the cell temperature is calculated, the DC power, including the ambient temperature effect, can be calculated as follows:

$$I_{mpp}^{Temp} = I_{mpp,ref}\left(1 + a\left(T_c - T_{ref}\right)\right)\frac{G}{G_{ref}} \tag{28}$$

$$V_{mpp}^{Temp} = V_{mpp, ref}\left(1 + b\left(T_c - T_{ref}\right)\right) \\ \times \ln\left(e + c\left(G - G_{ref}\right)\right) \tag{29}$$

$$P_{DC} = V_{mpp}I_{mpp} \tag{30}$$

The superscript *Temp* stands for ambient temperature-affected quantities.

As can be seen, the DC power in Fig. 10 is calculated for both with and without the effect of temperature. The main reason to calculate these two parameters is to identify an occurrence of overheating. The next step is calculating the AC power, which is realized

using the DC power and inverter data outputs. The AC power is calculated as follows [10]:

$$P_{ac} = \left(\frac{P_{aco}}{A - B} - C(A - B) \right) \left(P_{DC}^{Temp} - B \right)$$
$$+ C \left(P_{DC}^{Temp} - B \right)^2$$

(31)

$$A = P_{dco}(1 + C_1(V_{DC} - V_{dco}))$$

(32)

$$B = P_{so}(1 + C_2(V_{DC} - V_{dco}))$$

(33)

$$C = C_o(1 + C_3(V_{DC} - V_{dco}))$$

(34)

P_{aco} is the maximum AC-power rating for an inverter at reference or nominal operating condition, P_{dco} is the DC-power level at which the ac-power rating is achieved at the reference condition, V_{dco} DC-voltage level at which the ac-power rating is achieved at the reference operating condition, P_{so} is DC-power required to start the inversion process, or self-consumption by inverter, strongly influences inverter efficiency at low power levels, and C_0, C_1, C_2, and C_3 are constants.
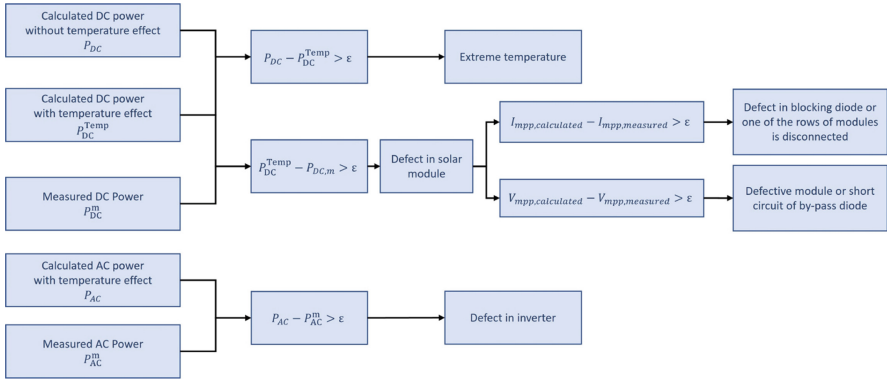
Fig. 11. Failure identification

Once the powers at AC and DC sides are calculated, they will be evaluated using the approach depicted in Fig. 11 to identify the failure.

5   Results

Dr. Solar employs an efficient web platform as the user interface where the user or the operator can check the measured values and implement desired settings. This section summarizes the input and output pages that the user/operator would be faced while working with Dr. Solar's solution.

5.1 Optimum Decision Support

Figure 12 depicts the input and output pages for the optimum decision support service of the Dr. Solar box. The input page acquires the daily fixed load and photovoltaic generation from Dr. Solar's measurements. The electricity prices are based on historical data. For the selected date, the user\operator is asked to choose the preference on including the battery storage system (if available) and electric vehicle (EV) (If available) in the optimization process. In addition, the availability of any other flexible load is also asked for and considered in the optimization process.
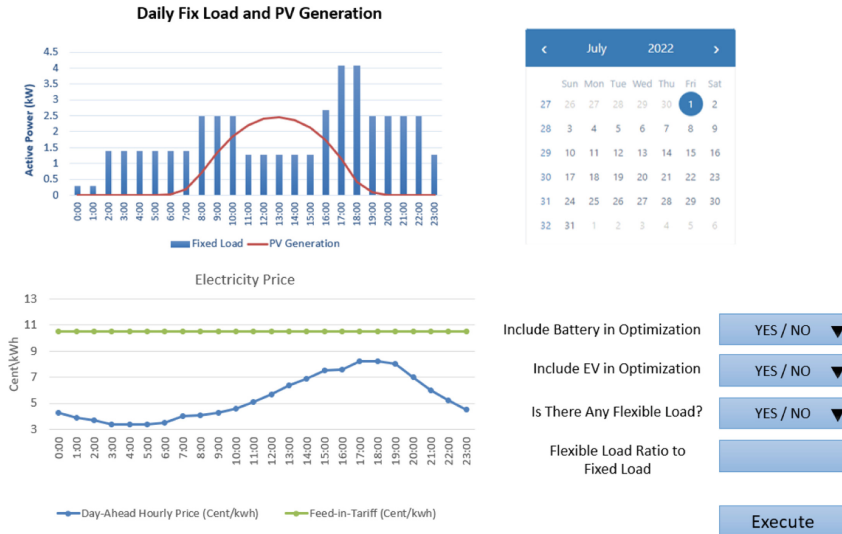
Fig. 12. The user interface for optimal decision support page: input page

The output page, i.e., Fig. 13, shows the optimum schedule offered by the optimum decision support algorithm and associated saving for the customer.
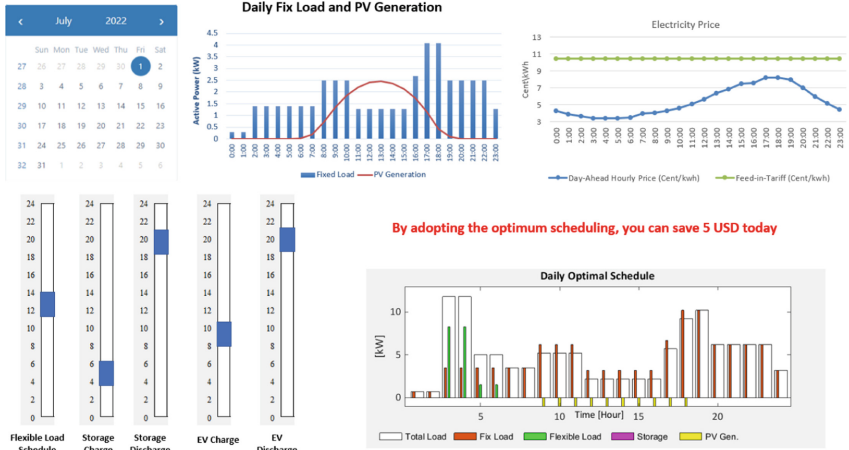
Fig. 13. The user interface for optimal decision support page: output page

5.2 Asset Management

Figure 14 depicts the inputs required for performing the asset management algorithms. The required inputs are based on the datasheet of the photovoltaic power plant, which the operator can easily access. Then, the asset management evaluation period is asked. At least three days are required for decision-making with an acceptable level of accuracy. When the evaluation is finished, the output page, as depicted in Fig. 15, will be shown to the operator/user. Here, the main output is the message which shows the potential deficiency in the solar photovoltaic system. The list of possible output messages is as follows:

- No failure is detected
- Defect in solar module

  - Defective module or short circuit of by-pass diode
  - A defect in the blocking diode or one of the rows of modules is disconnected

- Defect in inverter

Fig. 14. The user interface for the asset management page: input page
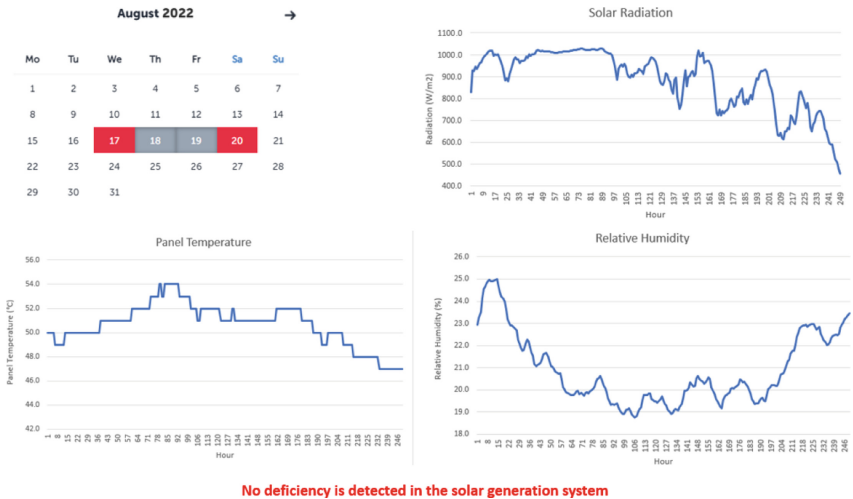

Fig. 15. The user interface for the asset management page: output page

6   Conclusion

This paper discusses the development of Dr. Solar, a sensor-based device for solar panel optimization and diagnostics. The device uses sensors to measure solar radiation, photovoltaic panel surface temperature, temperature, relative humidity, and position. The data collected by the Dr. Solar box is combined with data collected from the inverter and sent to a cloud service for processing. Using artificial intelligence algorithms, the data is analyzed, and the results are presented to the user through a web-based interface.

The results will provide the user with information on faults or degradations, as well as advice on optimizing adjustments of the physical position (tilt and angle).

6.1 Future Work

A companion paper (to be submitted) describes business model considerations. Another work in progress discusses neighborhood sentiments toward solar panel adoption based on aesthetics. For this research, we use a 3D household model with the possibility of adjusting tilt and angle.

References

1. SolarPower Europe: Global Market Outlook for Solar Power 05.2022. https://api.solarpowereurope.org/uploads/Solar_Power_Europe_Global_Market_Outlook_report_2022_2022_V2_07aa98200a.pdf
2. University of Michigan: Photovoltaic Energy Factsheet. https://css.umich.edu/publications/factsheets/energy/photovoltaic-energy-factsheet. Last accessed 19 Oct 2022
3. Dash, P.K., Gupta, N.C.: Effect of temperature on power output from different commercially available photovoltaic modules. Int. J. Eng. Res. Appl. **5**(1), 148–151 (2015)
4. Köntges, M., Kurtz, S., Packard, C., Jahn, U., Berger, K.A., Kato, K.: Performance and reliability of photovoltaic systems subtask 3.2: Review of failures of photovoltaic modules: IEA PVPS task 13: external final report IEA-PVPS. IEA. ISBN 978-3-906042-16-9 (2014)
5. Amajama, J., Oku, D.E.: Effect of relative humidity photovoltaic panels' output and solar illuminance/intensity. J. Sci. Eng. Res. **3**(4), 126–130 (2016)
6. Panjwani, M.K., Panjwani, S.K., Mangi, F.H., Khan, D., Meicheng, L.: Humid free efficient solar panel. In: 2nd International Conference on Energy Engineering and Smart Materials: ICEESM, vol. 1884, no. 1 (2017)
7. Teimourzadeh, S., Tor, O.B., Cebeci, M.E., Bara, A., Oprea, S.V.: A three-stage approach for resilience-constrained scheduling of networked microgrids. J. Mod. Power Syst. Clean Energy **7**(4), 705–715 (2019)
8. Cui, C., Zou, Y., Wei, L., Wang, Y.: Evaluating combination models of solar irradiance on inclined surfaces and forecasting photovoltaic power generation. IET Smart Grid **2**, 123–130 (2019)
9. Ciulla, G., Lo Brano, V., Moreci, E.: Forecasting the cell temperature of PV modules with an adaptive system. Int. J. Photoenergy **2013**, 1–10 (2013). https://doi.org/10.1155/2013/192854
10. Boyson, W.E., Galbraith, G.M., King, D.L., Gonz, S.: Performance Model for Grid-Connected Photovoltaic Inverters. Sandia National Laboratories (SNL), Albuquerque, NM, and Livermore, CA (2007)